ISSN (Print) 1226-1750
ISSN (Online) 2233-6656
Journal of Magnetics 24(3), 413-422 (2019) https://doi.org/10.4283/JMAG.2019.24.3.413

Structural, Half-metallic and Magnetic Properties of the Imperfect Pb_2FeReO_6 Containing Eight Different Inherent Defects

Yan Zhang[1]*, Hua-Xin Chen[1], Li Duan[1], Lei Ni[1], Ji-Bin Fan[1], Jie Wang[1], Guang-Teng Ci[1], and Vincent Ji[2]

[1]*School of Materials Science and Engineering, Chang'an University, Xi'an 710061, Shaanxi, China*
[2]*ICMMO/SP2M, UMR CNRS 8182, Université Paris-Sud, 91405 Orsay Cédex, France*

(Received 27 May 2019, Received in final form 12 September 2019, Accepted 17 September 2019)

The structural, half-metallic (HM) and magnetic properties of the imperfect Pb_2FeReO_6 containing eight different inherent defects of the Fe_{Re} or Re_{Fe} antisites, Fe1-Re1 or Fe1-Re4 interchanges, V_{Fe}, V_{Re}, V_O or V_{Pb} vacancies have been studied by first-principles calculations. No obvious structural changes are observed for Fe_{Re} or Re_{Fe} antisites, Fe1-Re1 or Fe1-Re4 interchanges and V_{Pb} vacancy defects, however, the six (two) nearest neighbors O (Fe or Re) of the vacancy move away from (close to) V_{Fe} or V_{Re} (V_O) vacancies. The HM character is maintained for Fe_{Re} or Re_{Fe} antisites, far Fe1-Re4 interchange, V_{Fe}, V_O or V_{Pb} vacancies, while vanished for near Fe1-Re1 interchange or V_{Re} vacancy. So the near Fe1-Re1 interchange or V_{Re} vacancy defects should be avoided to preserve the HM character of the Pb_2FeReO_6 and thus usable in spintronics devices. Except for the Fe_{Re} antisite case with a slightly higher total moment, the total moments μ_{tot} of the imperfect Pb_2FeReO_6 with the other seven inherent defects are smaller than 3.96 μ_B/f.u. of the perfect Pb_2FeReO_6.

Keywords : double perovskites, defects, half-metallic characters, magnetic properties, first-principles

1. Introduction

Based on the first-principles calculations on the semi-Heusler alloys NiMnSb and PtMnSb, the concept of half-metallic (HM) ferromagnets (FMs) was first proposed by Groot *et al.* [1] in 1983. Then, the HM magnetic materials immediately attracted much research in theory [2-10] and experiment [11-15] for their potential applications in magnetoelectronic [16] and spintronic [17] devices. Typical representations of the HM magnetic materials include spinel Fe_3O_4 [18, 19] and $FeCr_2S_4$ [20], rutile CrO_2 [21-23], Mn doping GaAs [24, 25], Ca doping single perovskite $La_{1-x}Ca_xMnO_3$ [26], double perovskites Sr_2FeMoO_6 [27] and Sr_2FeReO_6 [28]. The HM materials are characterized by the coexistence of metallic conducting behavior in one electron spin channel and insulating behavior in the other spin channel. Their electronic density of states (DOS) is completely (100%) spin polarized at the Fermi level, and conductivity is dominated by these metallic single-spin charge carriers. Therefore, the HM materials offer potential technological applications in the realm of single-spin electron source and high-efficiency magnetic sensors [16, 17].

The finding of the HM ferromagnetism, large tunneling magnetoresistance (TMR) and high Curie temperature (T_c) in Sr_2FeMoO_6 [27] and Sr_2FeReO_6 [28] by Kobayashi *et al.* in 1998 and 1999 revives the extensive study of the double perovskites, which are usually with a general chemical formula of $A_2MM'O_6$, where A is an alkaline-earth-metal atom (Ca, Sr or Ba) or a rare-earth-metal atom (La, Ce or Nd), M a 3*d* transition-metal (TM) atom (Cr, Mn, Fe, Co, Ni or Zn), M' a 4*d* TM atom (Mo, Te or Ru) or 5*d* TM atom (W, Re or Os). Besides experimental works [27, 28, 29-36], various first-principles calculation methods [27, 28, 37-42] including the local (spin) density approximation (L(S)DA) and the generalized gradient approximation (GGA), have been used to investigate the electronic and magnetic properties of the ordered Sr_2FeMoO_6 and Sr_2FeReO_6. The smaller saturation magnetizations of 3 and 2.7 μ_B per formula unit (f.u.) at 4.2 K for Sr_2FeMoO_6 [27] and Sr_2FeReO_6 [28] respectively, are attributed to the mis-site-type disorder of the TM atoms M and M' [43-45].

In 2009, a new double perovskite Pb_2FeReO_6 was successively prepared at 6 GPa and 1000 ºC by Nishimura *et al.* [46]. Despite the presence of Pb^{2+} ion at the A site, its

*Corresponding author: Tel: +862982337340
Fax: +862982337340, e-mail: yan.zhang@chd.edu.cn

crystal structure was determined to be a body-centered tetragonal (BCT) with a space group of I4/m and the lattice constants of a = b = 5.62 Å and c = 7.95 Å. Its Curie temperature (T_c) of 420 K is slightly higher than 401 K of Sr_2FeReO_6 [28] and its HM ferrimagnetic nature implies its potential application in magnetoelectronic and spintronic devices. Fabrication of the double perovskite Pb_2FeReO_6, either in bulk-sintered, single-crystalline, or epitaxial thin-film growth, would necessarily lead to a certain degree of imperfections. For instance, in their work on sintered Pb_2FeReO_6, Nishimura *et al.* [46] found that the saturation magnetization could be adjusted by using different heat treatment methods to change the degree of Fe^{3+}/Re^{5+} ordering. It is theoretically and experimentally shown that the ordering of the TM Fe and Mo/Re as well as the oxygen vacancy are the key factors determining the macroscopic magnetic properties of the Sr_2FeMoO_6 and Sr_2FeReO_6. The antisite defects, which are defined as the misplacement of Fe in Mo/Re positions and vice versa, and the oxygen vacancy generally decrease the saturation magnetization [27, 28, 47-54]. Therefore, in this paper, on the point of view of the HM character and magnetization reduction, the structural, electronic and magnetic properties of the imperfect Pb_2FeReO_6 containing eight different inherent defects of the Fe antisite (Fe_{Re}), Re antisite (Re_{Fe}), Fe1-Re1 interchange (Fe1-Re1), Fe1-Re4 interchange (Fe1-Re4), Fe vacancy (V_{Fe}), Re vacancy (V_{Re}), O vacancy (V_O) or Pb vacancy (V_{Pb}) have been studied by using first-principles projector augmented wave (PAW) within generalized gradient approximation as well as taking into account on-site Coulomb repulsive interaction (GGA+U). To the best of our knowledge, a systemic study on the effects of these inherent defects on the structural, electronic and magnetic properties of the Pb_2FeReO_6 has not been done up to now.

2. Calculation Method and Models

The calculations are performed using the Vienna *ab initio* simulation package (VASP) based on the density function theory (DFT) [55-58]. The interaction between electron and ionic core is represented by the projector augmented wave (PAW) potentials [59]. To treat electron exchange and correlation, we chose the Perdew-Burke-Ernzerhof (PBE) [60] formulation of the generalized gradient approximation (GGA) as well as taking into account the on-site Coulomb repulsive interaction (GGA+U) with the effective U parameters of 2.0 eV for Fe and 1.0 eV for Re [38, 40, 61], which yields the correct ground state of the strong correlation systems. A conjugate-gradient algorithm is used to relax the ions into their ground states, and the energies and the forces on each ion are converged within 1.0×10^{-4} eV/atom and 0.02 eV/Å, respectively. The cutoff energy for the plane-waves is chosen to be 450 eV. The Pb $6s^26p^2$, Fe $3d^64s^2$, Re $5d^56s^2$ and O $2s^22p^4$ electrons are treated as valence electrons. The k-point is sampled according to the Monkhorst-Pack automatic generation scheme with their origin at Γ point [62] together with a Gaussian smearing broadening of 0.1 eV.

In order to compare the imperfect and perfect Pb_2FeReO_6 on the same footing, the calculations are all performed by constructing a supercell of 4 f.u.. As compared with Fig. 1 (i) for the perfect $Pb_8Fe_4Re_4O_{24}$, eight different inherent defects (marked with stars) are considered here: (a) Fe_{Re} antisite at (0.5, 0.5, 0.5) site ($Pb_8Fe_5Re_3O_{24}$), (b) Re_{Fe} antisite at (0, 0.5, 0.5) site ($Pb_8Fe_3Re_5O_{24}$), (c) near Fe1-Re1 interchange at (0, 0, 0) and (0, 0, 0.5) sites ($Pb_8Fe_4Re_4O_{24}$), (d) farther Fe1-Re4 interchange at (0, 0, 0) and (0.5, 0.5, 0.5) sites ($Pb_8Fe_4Re_4O_{24}$), (e) V_{Fe} vacancy at (0, 0.5, 0.5) site ($Pb_8Fe_3Re_4O_{24}$), (f) V_{Re} vacancy at (0.5, 0.5, 0.5) site ($Pb_8Fe_4Re_3O_{24}$), (g) V_O vacancy at (0.5, 0.5, 0.25) site ($Pb_8Fe_4Re_4O_{23}$) and (h) V_{Pb} vacancy at (0.75, 0.75, 0.75) site ($Pb_7Fe_4Re_4O_{24}$).

3. Results and Discussions

3.1. Optimized structures

The optimized structures of 4 f.u. Pb_2FeReO_6 with eight different inherent defects (marked with stars) are shown in Figs. 1(a)-(h) together with the perfect one (i) for comparison. From Figs. 1(a), (b), (c), and (d) we can see that, in Fe_{Re} or Re_{Fe} antisites, Fe1-Re1 or Fe1-Re4 interchanges cases, no obvious structural changes are observed due to Fe^{3+} and Re^{5+} ions having similar radii of 0.78 and 0.72 Å [63], respectively. However, from Fig. 1(e) [(f)] we can see that, a V_{Fe} [V_{Re}] vacancy makes its six nearest neighbor oxygen atoms move close to their nearest Re [Fe] neighbors, so that the corresponding Re-O [Fe-O] bond lengths reduce to 1.906 Å [1.844 Å] (ab plane) and 1.909 Å [1.846 Å] (c axis). While in the perfect Pb_2FeReO_6 as shown in Fig. 1 (i), the optimized Re-O [Fe-O] bond lengths are 1.934 Å [2.019 Å] (ab plane) and 1.944 Å [2.021 Å] (c axis). This is because a V_{Fe} [V_{Re}] vacancy loses the attraction force to its six nearest neighbor oxygen atoms from a removed Fe [Re] atom. On the contrary, Fig. 1(g) shows a V_O vacancy leads its nearest neighbor TM atoms Fe and Re move close to V_O vacancy site, so that the corresponding Fe-Re distance reduces to 3.452 Å (c axis), which is much smaller than Fe-Re distance of 3.965 Å (c axis) in the perfect Pb_2FeReO_6 case. The reason may be that the larger distance of 3.452

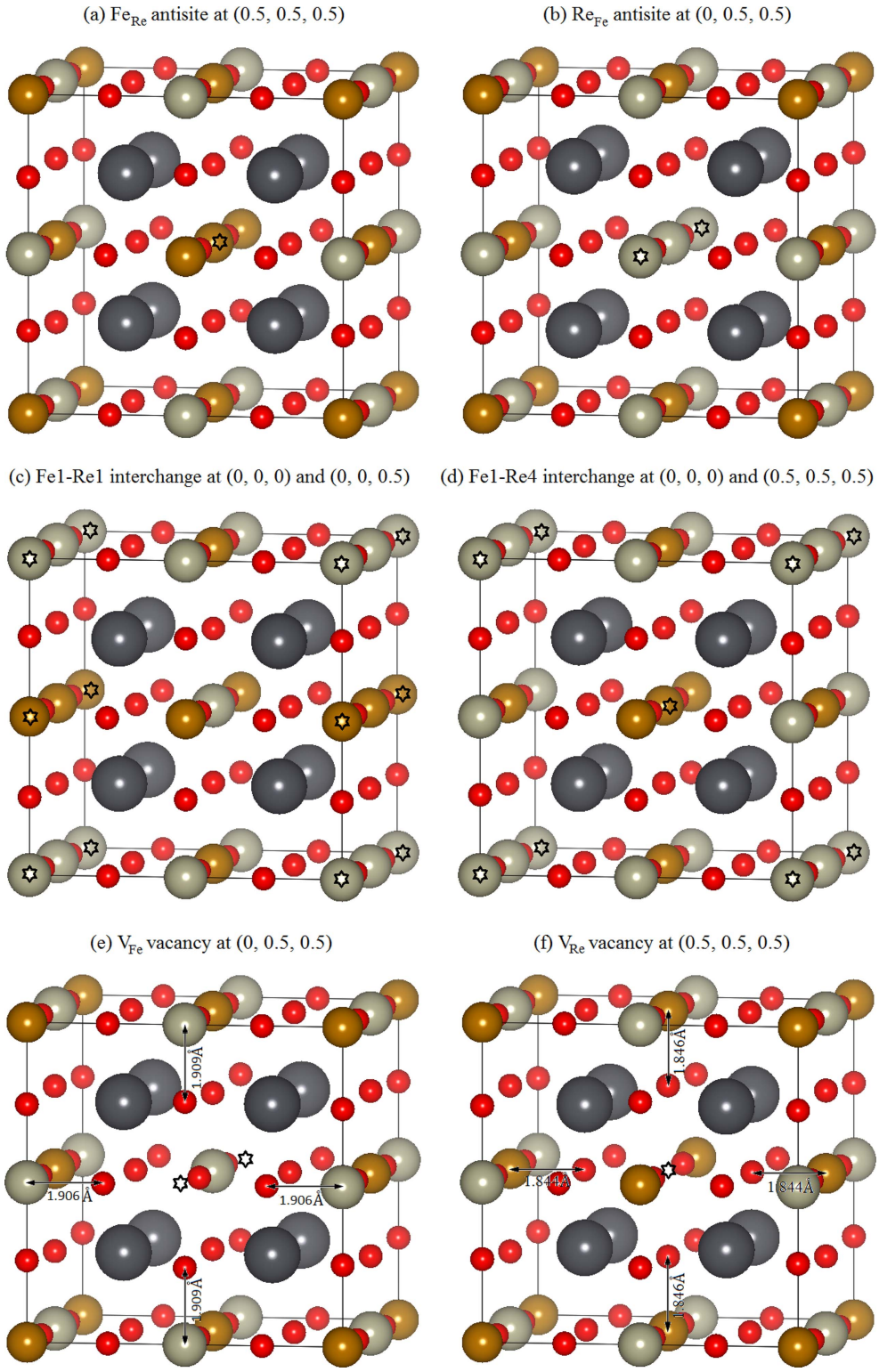

Fig. 1. (Color online) The optimized structures of imperfect (marked with stars) Pb_2FeReO_6 with (a) Fe_{Re} antisite, one Fe atom substitutes for one Re atom at (0.5, 0.5, 0.5) site ($Pb_8Fe_5Re_3O_{24}$); (b) Re_{Fe} antisite, one Re atom substitutes for one Fe atom at (0, 0.5, 0.5) site ($Pb_8Fe_3Re_5O_{24}$), (c) Fe1-Re1 interchange, exchange Fe and Re positions respectively at (0, 0, 0) and (0, 0, 0.5) sites ($Pb_8Fe_4Re_4O_{24}$), (d) Fe1-Re4 interchange, exchange Fe and Re positions respectively at (0, 0, 0) and (0.5, 0.5, 0.5) sites ($Pb_8Fe_4Re_4O_{24}$), (e) V_{Fe} vacancy, removing one Fe atom from (0, 0.5, 0.5) site ($Pb_8Fe_3Re_4O_{24}$), (f) V_{Re} vacancy, removing one Re atom from (0.5, 0.5, 0.5) site ($Pb_8Fe_4Re_3O_{24}$), (g) V_O vacancy, removing one O atom from (0.5, 0.5, 0.25) site ($Pb_8Fe_4Re_4O_{23}$), (h) V_{Pb} vacancy, removing one Pb atom from (0.75, 0.75, 0.75) site ($Pb_7Fe_4Re_4O_{24}$), and (i) Perfect one ($Pb_8Fe_4Re_4O_{24}$).

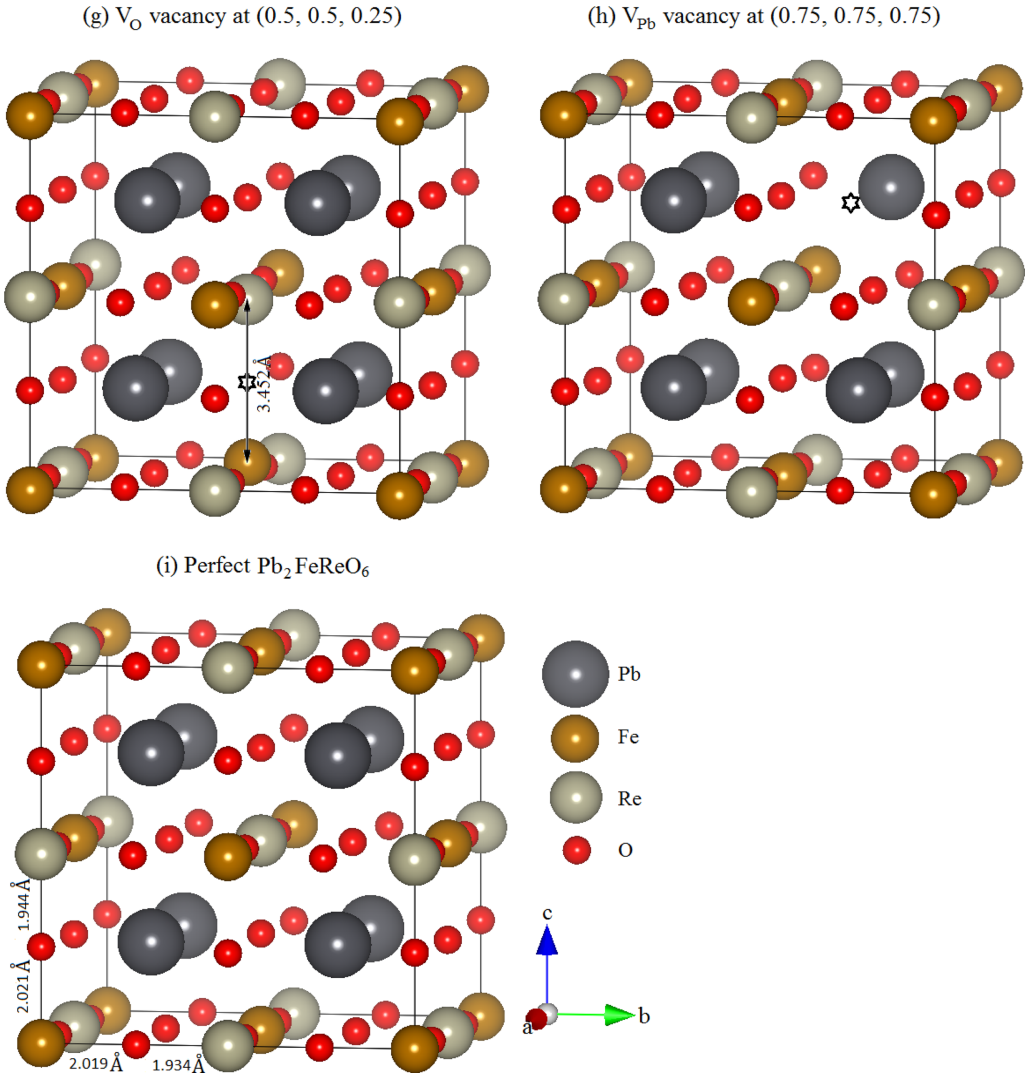

Fig. 1. Continued.

Å (c axis) leads to an attraction force between the Fe and Re atoms without middle oxygen atom. While Fig. 1(h) shows that there is also no obvious structural change for V_{Pb} vacancy case. This is because the interactions between Pb atom and the other nearest neighbor atoms are very weak.

3.2. Half-metallic characters

In order to investigate the effects of eight different inherent defects shown in Figs. 1(a)-(h) on the HM character of the double perovskite Pb_2FeReO_6, Fig. 2 shows the total density of states (TDOS) of 4 f.u. Pb_2FeReO_6 containing eight different defects of (a) Fe_{Re} antisite, (b) Re_{Fe} antisite, (c) Fe1-Re1 interchange, (d) Fe1-Re4 interchange, (e) V_{Fe} vacancy, (f) V_{Re} vacancy, (g) V_O vacancy, or (h) V_{Pb} vacancy. We can see that, the HM characters are maintained for imperfect Pb_2FeReO_6 containing (a) Fe_{Re} antisite, (b) Re_{Fe} antisite, (d) Fe1-Re4 interchange, (e) V_{Fe} vacancy, (g) V_O vacancy, or (h) V_{Pb} vacancy, because their down-spin channels (red lines) cross the Fermi level E_F and the up-spin channels (black lines) open the band gaps $E_g^{up\text{-}spin}$ of 1.347, 0.649, 0.567, 1.125, 0.761 and 1.249 eV, respectively. On the contrary, the HM characters are lost for imperfect Pb_2FeReO_6 containing (c) Fe1-Re1 interchange and (f) V_{Re} vacancy, since the TDOS of both channels cross the Fermi level E_F. The HM character of the imperfect Pb_2FeReO_6 is lost for (c) Fe1-Re1 interchange at (0, 0, 0) and (0, 0, 0.5) sites but is maintained for (d) Fe1-Re4 interchange at (0, 0, 0) and (0.5, 0.5, 0.5) sites are obviously because the separation distance of 3.965 Å for Fe1-Re1 interchange is smaller than that of 6.856 Å for Fe1-Re4 interchange. So we conclude that the near Fe1-Re1 interchange and V_{Re} vacancy defects should be avoided to preserve the HM

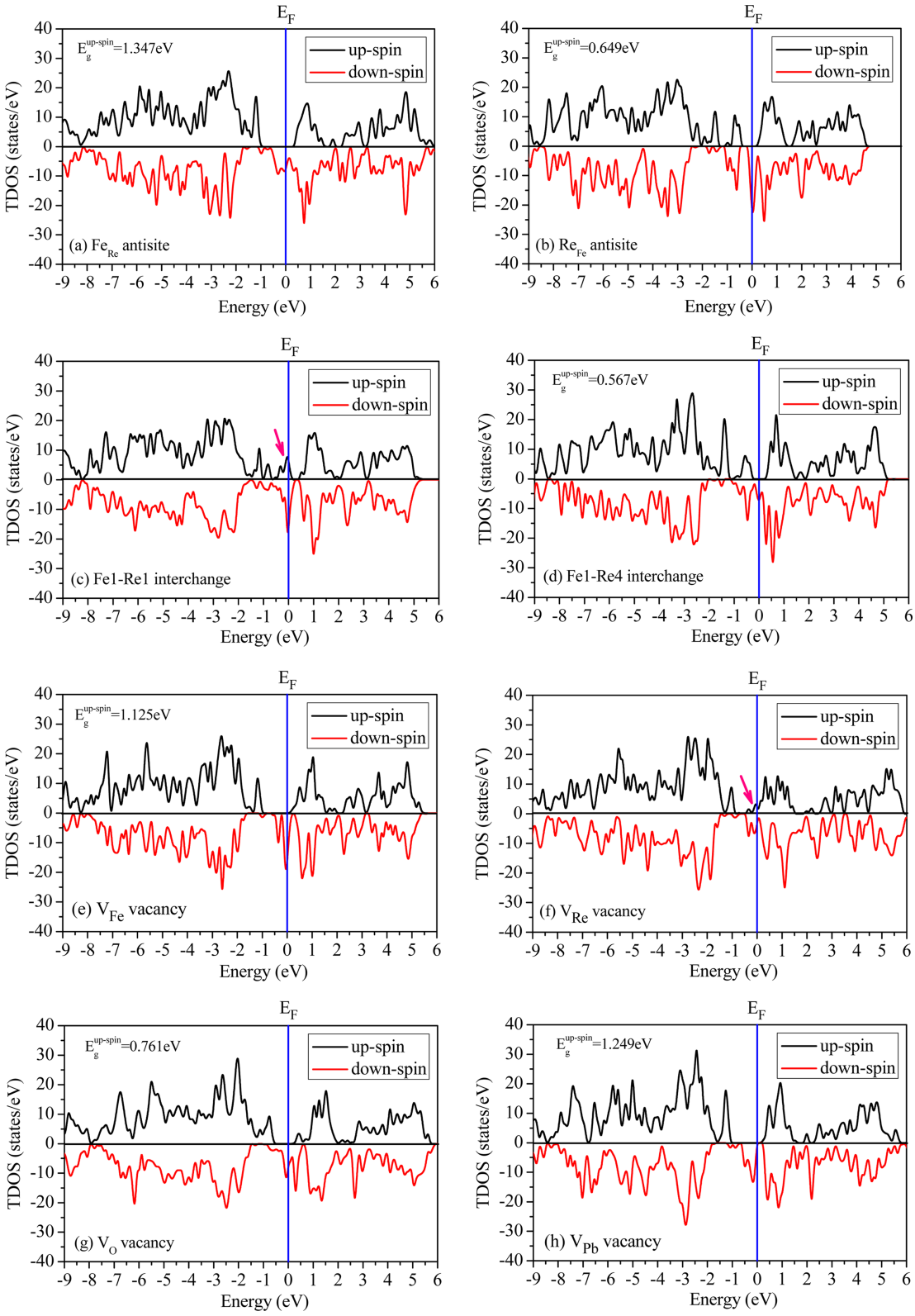

Fig. 2. (Color online) Total density of states (TDOS) of imperfect Pb_2FeReO_6 containing eight different defects of (a) Fe_{Re} antisite, (b) Re_{Fe} antisite, (c) Fe1-Re1 interchange, (d) Fe1-Re4 interchange, (e) V_{Fe} vacancy, (f) V_{Re} vacancy, (g) V_O vacancy, and (h) V_{Pb} vacancy. The black and red lines represent up-spin and down-spin channels, respectively, and the Fermi level E_F is set at zero energy and indicated by vertical blue lines.

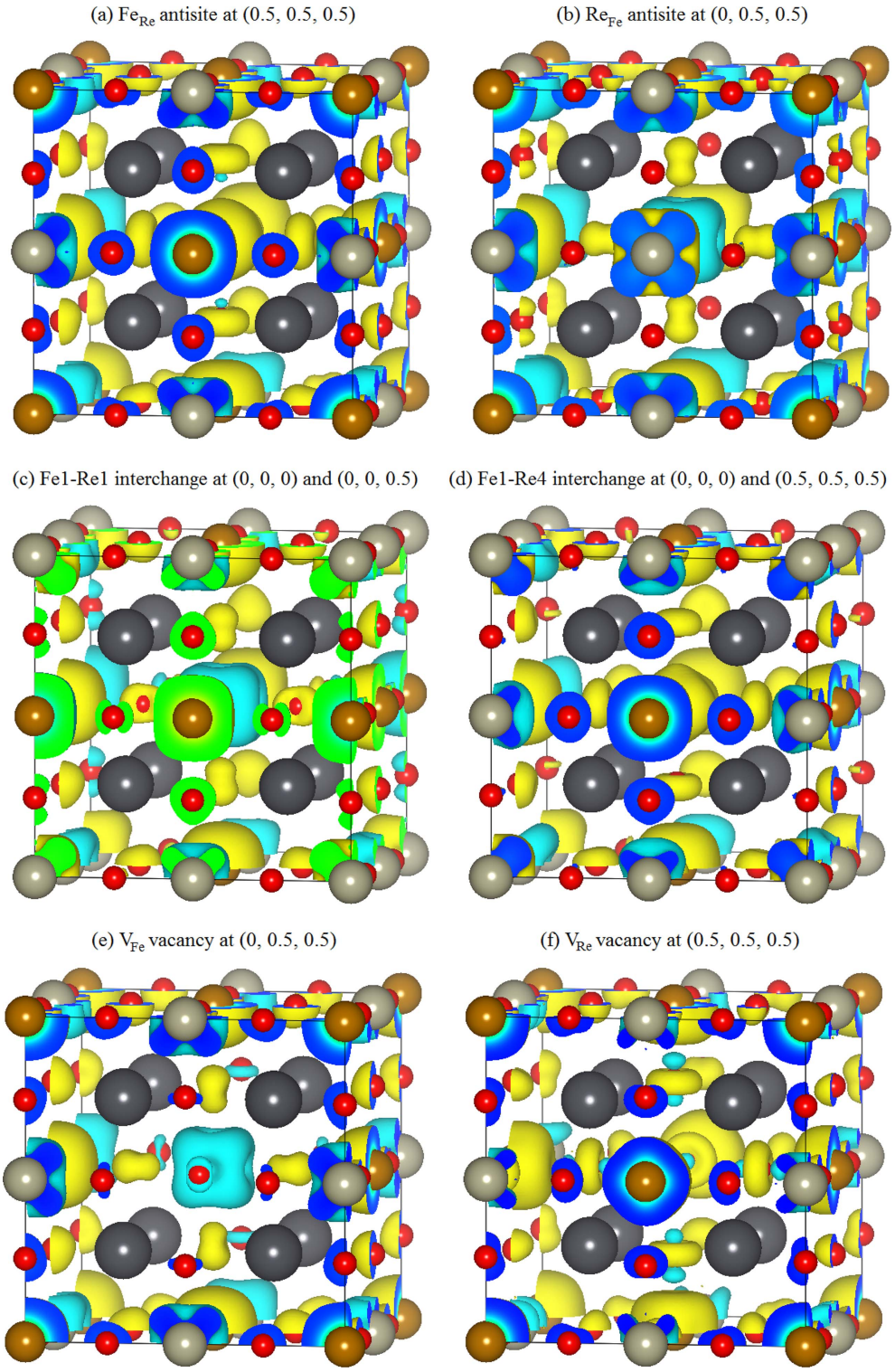

Fig. 3. (Color online) The difference/spin charge density of imperfect Pb_2FeReO_6 containing eight different defects of (a) Fe_{Re} antisite at (0.5, 0.5, 0.5) site, (b) Re_{Fe} antisite at (0, 0.5, 0.5) site, (c) Fe1-Re1 interchange at (0, 0, 0) and (0, 0, 0.5) sites, (d) Fe1-Re4 interchange at (0, 0, 0) and (0.5, 0.5, 0.5) sites, (e) V_{Fe} vacancy at (0, 0.5, 0.5) site, (f) V_{Re} vacancy at (0.5, 0.5, 0.5) site, (g) V_O vacancy at (0.5, 0.5, 0.25) site, or (h) V_{Pb} vacancy at (0.75, 0.75, 0.75) site. The difference/spin charge density of the perfect Pb_2FeReO_6 of 4 f.u. is also shown in (i) for comparison. The yellow (turquoise) isosurfaces represent positive (negative) charge density of 0.005/Å^3 and thus up-spin (down-spin) moment. In the (100) cross sections, the colors blue, turquoise and green represent the value of charge density in increasing order.

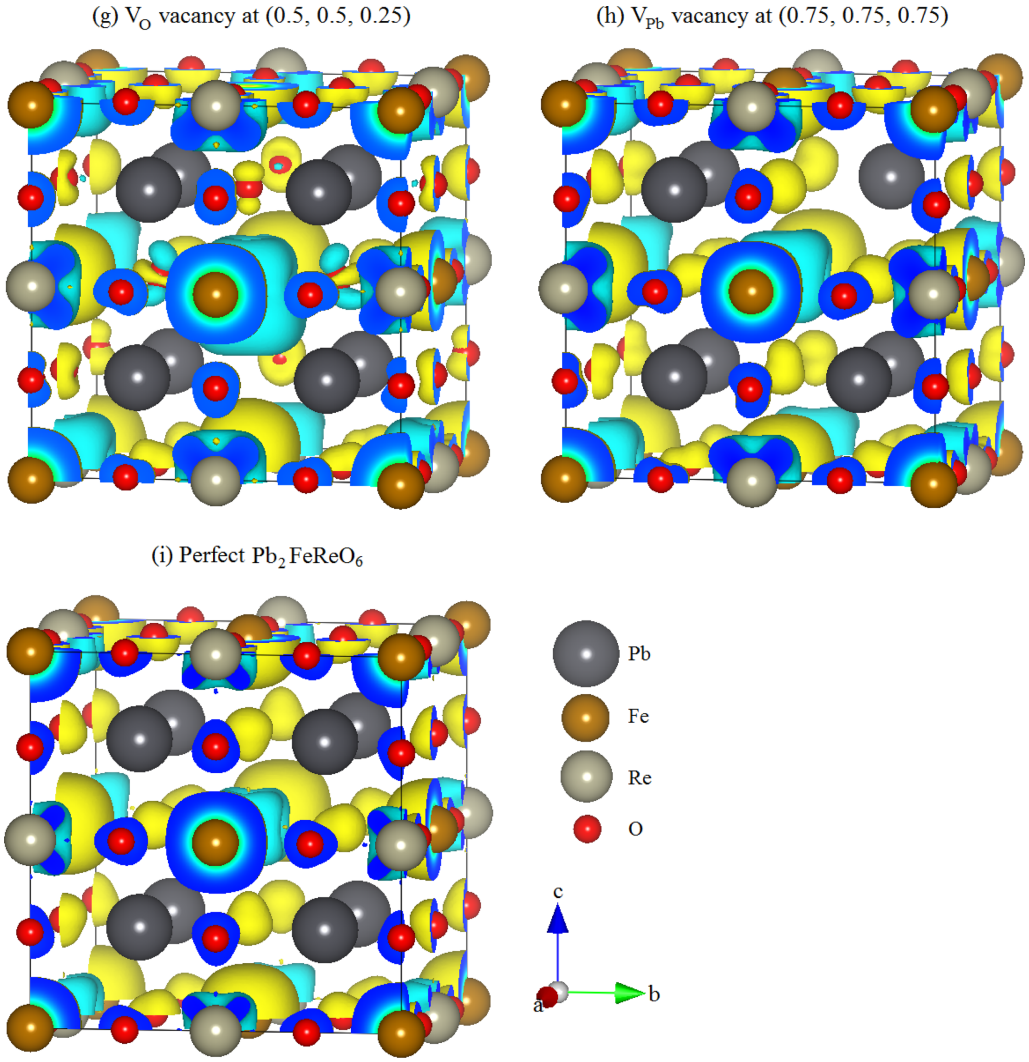

Fig. 3. Continued.

character of the Pb_2FeReO_6 and thus usable in spintronics devices.

3.3. Magnetic couplings and moments

In order to investigate the effects of eight different inherent defects shown in Figs. 1(a)-(h) and the TDOS shown in Figs. 2(a)-(h) on the magnetic couplings and moments, the difference/spin charge densities are shown in Fig. 3 for imperfect Pb_2FeReO_6 of 4 f.u. containing eight different defects of (a) Fe_{Re} antisite at (0.5, 0.5, 0.5) site, (b) Re_{Fe} antisite at (0, 0.5, 0.5) site, (c) Fe1-Re1 interchange at (0, 0, 0) and (0, 0, 0.5) sites, (d) Fe1-Re4 interchange at (0, 0, 0) and (0.5, 0.5, 0.5) sites, (e) V_{Fe} vacancy at (0, 0.5, 0.5) site, (f) V_{Re} vacancy at (0.5, 0.5, 0.5) site, (g) V_O vacancy at (0.5, 0.5, 0.25) site, or (h) V_{Pb} vacancy at (0.75, 0.75, 0.75) site. The difference/spin charge density of the perfect Pb_2FeReO_6 of 4 f.u. is also shown in (i) for comparison. We can see that firstly, similar to the perfect Pb_2FeReO_6 case, each of the two TM atoms Fe and Re on regular sites are ferromagnetic (FM) arranged within each sublattice, while the two sublattices are coupled anti-ferromagnetic (AFM). Second, in (a) Fe_{Re} antisite at (0.5, 0.5, 0.5) site ((b) Re_{Fe} antisite at (0, 0.5, 0.5) site) cases, an FM (AFM) coupling is obtained between Fe_{Re} (Re_{Fe}) antisite and regular Fe (Re) sites, in (c) Fe1-Re1 interchange at (0, 0, 0) and (0, 0, 0.5) sites, an AFM coupling is observed between Fe_{Re} (Re_{Fe}) antisite and regular Fe (Re) sites, while in (d) Fe1-Re4 interchange at (0, 0, 0) and (0.5, 0.5, 0.5) sites, the spin moment of Fe (Re) cation situated on Re (Fe) antisite is coupled FM (AFM) with those of Fe (Re) cations on the regular sites. Thirdly, as expected each cation defect affects mainly its six nearest neighbor oxygen atoms. In cases of (a) Fe_{Re} antisite, (c) Fe1-Re1 interchange, (d) Fe1-Re4

interchange, (e) V_{Fe} vacancy, or (f) V_{Re} vacancy, a partial negative spin moment (turquoise) presents on the six nearest neighbor oxygen atoms, while in (b) Re_{Fe} antisite case, no spin moments are observed on its six nearest neighbor oxygen atoms. Fourth, in (g) a V_O vacancy at (0.5, 0.5, 0.25) site causes the nearest neighbor Re4 cation at central (0.5, 0.5, 0.5) site a much large and expansive negative spin moment (turquoise) and its five survived nearest neighbor oxygen atoms a partial negative spin moment (turquoise). Finally, both no spin density distributions at eight Sr sites in (a)-(g) and no obvious influence on the magnetic moment distributions in (h) V_{Pb} vacancy case indicate the magnetic moment contributions of Pb atoms are neglectable.

The initial fractional coordinates (x, y, z) and atomic local magnetic moments μ (μ_B) of the Fe and Re atoms on regular sites and antisites, the total magnetic moments μ_{tot} (μ_B/f.u.), HM characters and up-spin band gaps $E_g^{up\text{-}spin}$ (eV) of the imperfect Pb_2FeReO_6 of 4 f.u. containing eight different defects are summarized in Table 1 together with the values of the perfect Pb_2FeReO_6 for comparison. We can see that for Fe_{Re} antisite case, the largest total moment 4.22 μ_B/f.u. is resulted from the occurrence of parallel aligned moment 1.913 μ_B on Fe_{Re} antisite. For Re_{Fe} antisite case, the reduced saturation magnetization is attributed to the supplied parallel aligned moment 1.199 μ_B by Re_{Fe} antisite is smaller than the disappeared moment 3.929 μ_B of the substituted Fe. In Fe1-Re1 (Fe1-Re4) interchange cases, antiparallel (parallel) aligned moments –3.851 μ_B (1.514 μ_B) on Fe_{Re} antisites and supplied smaller parallel aligned moments 0.962 μ_B (0.877 μ_B) by Re_{Fe} antisites lead to the lowest (lower) saturation magnetizations 1.94 μ_B/f.u. (3.44 μ_B/f.u.) than the perfect one. The vanishing of a Fe atom and thus its parallel aligned moment 3.929 μ_B is clearly responsible for the reduced saturation magnetization of the imperfect Pb_2FeReO_6 with V_{Fe} vacancy. Although removing a Re atom leads to a vanishing (decreasing) antiparallel aligned moments on itself (its three near Re1, Re2 and Re3 neighbors) and a slightly increasing parallel aligned moment on the Fe1 atom, the decreasing parallel aligned moments on its three near Fe2, Fe3 and Fe4 neighbors result in a smaller saturation magnetization of 3.67 μ_B/f.u. for imperfect Pb_2FeReO_6 with V_{Re} vacancy. Removing an oxygen atom and thus its parallel aligned moment causes slightly decreasing parallel aligned moments on four Fe atoms and increasing antiparallel aligned moments on four Re atoms lead to a smaller saturation magnetization of 3.04 μ_B/f.u. for the imperfect Pb_2FeReO_6 containing V_O vacancy. Although removing a Pb atom leads to a decreasing antiparallel aligned moments of four Re atoms, the decreasing parallel aligned moments on four Fe atoms

Table 1. The initial fractional coordinates (x, y, z) and atomic magnetic moment μ (μ_B) of Fe and Re atoms on regular sites and antisites, the total magnetic moment μ_{tot} (μ_B/f.u.), HM character and up-spin band gap $E_g^{up\text{-}spin}$ (eV) of the imperfect Pb_2FeReO_6 with four f.u. and eight different defects. The values corresponding to the perfect Pb_2FeReO_6 are also listed in the last column for comparison.

Atoms	Sites	(x, y, z)	Fe_{Re}	Re_{Fe}	Fe1-Re1	Fe1-Re4	V_{Fe}	V_{Re}	V_O	V_{Pb}	Perfect
Fe	regular sites	Fe1(0, 0, 0)	3.866	3.848	Re_{Fe}	Re_{Fe}	3.828	3.949	3.811	3.811	3.929
		Fe2(0, 0.5, 0.5)	3.777	Re_{Fe}	3.842	3.793	V_{Fe}	3.336	3.801	3.838	3.929
		Fe3(0.5, 0, 0.5)	3.761	3.846	3.848	3.812	3.848	3.210	3.810	3.831	3.929
		Fe4(0.5, 0.5, 0)	3.770	3.848	3.856	3.823	3.865	3.237	3.648	3.834	3.929
	antisites	Fe_{Re}(0.5, 0.5, 0.5)	1.913 Fe_{Re}			1.514 Fe_{Re}					
		Fe_{Re}(0, 0, 0.5)			-3.851 Fe_{Re}						
Re	regular sites	Re1(0, 0, 0.5)	-0.626	-0.917	Fe_{Re}	-0.467	-0.628	-0.120	-0.840	-0.607	-0.831
		Re2(0, 0.5, 0)	-0.509	-0.945	-0.351	-0.454	-0.631	-0.117	-0.881	-0.609	-0.831
		Re3(0.5, 0, 0)	-0.514	-1.275	-0.320	-0.438	-0.348	-0.109	-0.883	-0.606	-0.831
		Re4(0.5, 0.5, 0.5)	Fe_{Re}	-0.953	-1.015	Fe_{Re}	-0.615	V_{Re}	-1.231	-0.616	-0.831
	antisites	Re_{Fe}(0, 0.5, 0.5)		1.199 Re_{Fe}							
		Re_{Fe}(0, 0, 0)			0.962 Re_{Fe}	0.877 Re_{Fe}					
μ_{tot}			4.22	2.32	1.94	3.44	2.54	3.67	3.04	3.52	3.96
HM			yes	yes	no	yes	yes	no	yes	yes	yes
$E_g^{up\text{-}spin}$			1.374	0.649	-	0.567	1.125	--	0.761	1.249	1.240

results in a smaller total moment of 3.52 μ_B/f.u. for imperfect Pb_2FeReO_6 with V_{Pb} vacancy. In conclusion, except for the Fe_{Re} antisite case with a slightly higher total moment, the total moments μ_{tot} of the imperfect Pb_2FeReO_6 with the other seven inherent defects are smaller than 3.96 μ_B/f.u. of the perfect Pb_2FeReO_6.

4. Conclusions

In point of view of the HM character and magnetization reduction, the structural, electronic and magnetic properties of the imperfect Pb_2FeReO_6 containing eight different inherent defects of Fe_{Re} or Re_{Fe} antisites, Fe1-Re1 or Fe1-Re4 interchanges, V_{Fe}, V_{Re}, V_O or V_{Sr} vacancies have been studied by using the first-principles projector augmented wave (PAW) potential within the generalized gradient approximation as well as taking into account on-site Coulomb repulsive interaction (GGA+U). Following conclusions have been obtained.

1. No obvious structural changes are observed for the imperfect Pb_2FeReO_6 containing Fe_{Re} or Re_{Fe} antisites, Fe1-Re1 or Fe1-Re4 interchanges, and V_{Pb} vacancy defects, however, the six (two) nearest neighbors O (Fe or Re) of the vacancy move away from (close to) V_{Fe} or V_{Re} (V_O) vacancies.

2. The HM character is maintained for the imperfect Pb_2FeReO_6 containing Fe_{Re} or Re_{Fe} antisites, far Fe1-Re4 interchange, V_{Fe}, V_O or V_{Pb} vacancies, while vanished when the near Fe1-Re1 interchange or V_{Re} vacancy are presented. So the near Fe1-Re1 interchange or V_{Re} vacancy defects should be avoided to preserve the HM character of the Pb_2FeReO_6 and thus usable in spintronics devices.

3. Except for the Fe_{Re} antisite case with a slightly higher total moment, the total moments μ_{tot} of the imperfect Pb_2FeReO_6 with the other seven inherent defects are smaller than 3.96 μ_B/f.u. of the perfect Pb_2FeReO_6.

Acknowledgments

The authors would like to acknowledge the National Natural Science Foundation of China (Grant Nos. 51501017, 61604016) and the Fundamental Research Funds for the Central Universities of Chang'an University (Grant Nos. 310831171013, 300102319103, CHD2017ZD142) for providing financial support for this research.

References

[1] R. A. de Groot, F. M. Müeller, P. G. van Engen, and H. J. Buschow, Phys. Rev. Lett. **50**, 2024 (1983).
[2] A. Yanase and K. Siratori, J. Phys. Soc. Jpn. **53**, 312 (1984).
[3] S. Fujii, S. Sugimura, S. Ishida, and S. Asano, J. Phys.: Condens. Matter. **2**, 8583 (1990).
[4] S. Picozzi, A. Continenza, and J. Freeman, Phys. Rev. B **66**, 094421 (2002).
[5] A. Yamasaki, L. Chioncel, A. I. Lichtenstein, and O. K. Andersen, Phys. Rev. B **74**, 024419 (2006).
[6] M. Sargolzaei, M. Richter, K. Koepernik, I. Opahle, H. Eschrig, and I. Chaplygin, Phys. Rev. B **74**, 224410 (2006).
[7] J. Kübler, G. H. Fecher, and C. Felser, Phys. Rev. B **76**, 024414 (2007).
[8] A. T. Zayak, P. Entel, and J. R. Chelikowsky, Phys. Rev. B **77**, 212401 (2008).
[9] P. Buczek, A. Ernst, P. Bruno, and L. M. Sandratskii, Phys. Rev. Lett. **102**, 247206 (2009).
[10] L. Y. Chen, S. F. Wang, Y. Zhang, J. M. Zhang, and K. W Xu, Thin Solid Films **519**, 4400 (2011).
[11] T. Ambrose, J. J. Krebs, and G. A. Prinz, J. Appl. Phys. **87**, 5463 (2000).
[12] N. D. Telling, P. S. Keatley, G. van der Laan, R. J. Hicken, E. Arenholz, Y. Sakuraba, M. Oogane, Y. Ando, K. Takanashi, A. Sakuma, and T. Miyazaki, Phys. Rev. B **78**, 184438 (2008).
[13] M. Kallmayer, P. Klaer, H. Schneider, E. A. Jorge, C. Herbort, G. Jakob, M. Jourdan, and H. J. Elmers, Phys. Rev. B **80**, 020406 (2009).
[14] P. Klaer, M. Kallmayer, C. G. F. Blum, T. Graf, J. Barth, B. Balke, G. H. Fecher, C. Felser, and H. J. Elmers, Phys. Rev. B **80**, 144405 (2009).
[15] K. Hild, J. Maul, G. Schönhense, and H. J. Elmers, Phys. Rev. Lett. **102**, 057207 (2009).
[16] G. A. Prinz, Science **282**, 1660 (1998).
[17] S. A. Wolf, D. D. Awschalom, R. A. Buhrman, J. M. Daughton, S. V. Molnár, M. L. Roukes, A. Y. Chtchelkanova, and D. M. Treger, Science **294**, 1488 (2001).
[18] Y. S. Dedkov, U. Rüdiger, and G. Güntherodt, Phys. Rev. B **65**, 064417 (2002).
[19] H. T. Jeng and G. Y. Guo, Phys. Rev. B **65**, 094429 (2002).
[20] M. S. Park, S. K. Kwon, S. J. Youn, and B. I. Min, Phys. Rev. B **59**, 10018 (1999).
[21] K. Schwarz, J. Phys. F: Met. Phys. **16**, L211 (1986).
[22] I. Mazin, D. J. Singh, and C. A. Draxl, Phys. Rev. B **59**, 411 (1999).
[23] S. M. Watts, S. Wirth, S. von Molnár, A. Barry, and J. M. D. Coey, Phys. Rev. B **61**, 9621 (2000).
[24] M. Shirai, T. Ogawa, I. Kitagawa, and N. Suzuki, J. Magn. Magn. Mater. **177-181**, 1383 (1998).
[25] J. H. Park, S. K. Kwon, and B. I. Min, Physica B **281-282**, 703 (2000).
[26] W. E. Pickett and D. J. Singh, Phys. Rev. B **53**, 1146 (1996).
[27] K. I. Kobayashi, T. Kimura, H. Sawada, K. Terakura, and Y. Tokura, Nature **395**, 677 (1998).
[28] K. I. Kobayashi, T. Kimura, Y. Tomioka, H. Sawada, K.

Terakura, and Y. Tokura, Phys. Rev. B **59**, 11159 (1999).
[29] Y. Tomioka, T. Okuda, Y. Okimoto, R. Kumai, K. I. Kobayashi, and Y. Tokura, Phys. Rev. B **61**, 422 (2000).
[30] O. Chmaissem, R. Kruk, B. Dabrowski, D. E. Brown, X. Xiong, S. Kolesnik, J. D. Jorgensen, and C. W. Kimball, Phys. Rev. B **62**, 14197 (2000).
[31] J. Navarro, C. Frontera, Ll. Balcells, B. Martínez, and J. Fontcuberta, Phys. Rev. B **64**, 092411 (2001).
[32] M. S. Moreno, J. E. Gayone, M. Abbate, A. Caneiro, D. Niebieskikwiat, R. D. Sánchez, A.de Siervo, R. Landers, and G. Zampieri, Physica B **320**, 43 (2002).
[33] A. Jung, V. Ksenofontov, S. Reiman, H. A. Therese, U. Kolb, C. Felser, and W. Tremel, Phys. Rev. B **73**, 144414 (2006).
[34] A. Jung, I. Bonn, V. Ksenofontov, M. Panthöfer, S. Reiman, C. Felser, and W. Tremel, Phys. Rev. B **75**, 184409 (2007).
[35] K. Ohno, H. Kato, T. Nishioka, and M. Matsumura, J. Magn. Magn. Mater. **310**, e666 (2007).
[36] Y. C. Hu, J. J. Ge, Q. Ji, Z. S. Jiang, X. S. Wu, and G. F. Cheng, Mater. Chem. Phys. **124**, 274 (2010).
[37] D. D. Sarma, P. Mahadevan, T. Saha-Dasgupta, S. Ray, and A. Kumar, Phys. Rev. Lett. **85**, 2549 (2000).
[38] Y. Moritomo, Sh. Xu, T. Akimoto, A. Machida, N. Hamada, K. Ohoyama, E. Nishibori, M. Takata, and M. Sakata, Phys. Rev. B **62**, 14224 (2000).
[39] Z. Fang, K. Terakura, and J. Kanamori, Phys. Rev. B **63**, 180407 (2001).
[40] H. Wu, Phys. Rev. B **64**, 125126 (2001).
[41] I. V. Solovyev, Phys. Rev. B **65**, 144446 (2002).
[42] H. T. Jeng and G. Y. Guo, Phys. Rev. B **67**, 094438 (2003).
[43] T. Saha-Dasgupta and D. D. Sarma, Phys. Rev. B **64**, 064408 (2001).
[44] A. S. Ogale, S. B. Ogale, R. Ramesh, and T. Venkatesan, Appl. Phys. Lett. **75**, 537 (1999).
[45] S. Ray, A. Kumar, D. D. Sarma, R. Cimino, S. Turchini, S. Zennaro, and N. Zema, Phys. Rev. Lett. **87**, 097204 (2001).
[46] K. Nishimura, M. Azuma, S. Hirai, M. Takano, and Y. Shimakawa, Inorg. Chem. **48**, 5962 (2009).
[47] A. B. Munoz-Garciıa, M. Pavone, and E. A. Carter, Chem. Mater. **23**, 4525 (2011).
[48] R. Kircheisen and J. Töpfer, J. Solid State Chem. **185**, 76 (2012).
[49] C. Meneghini, S. Ray, F. Liscio, F. Bardelli, S. Mobilio, and D. D. Sarma, Phys. Rev. Lett. **103**, 046403 (2009).
[50] L. Balcells, J. Navarro, M. Bibes, A. Roig, B. Martinez, and J. Fontcuberta, Appl. Phys. Lett. **78**, 781 (2001).
[51] X. F. Zhu, Q. F. Li, and L. F. Chen, Solid State Commun. **144**, 230 (2007).
[52] D. Stoeffler and S. Colis, J. Magn. Magn. Mater. **290-291**, 400 (2005).
[53] D. Stoeffler and S. Colis, Mater. Sci. Eng. B **126**, 133 (2006).
[54] D. Stoeffler and C. Etz, J. Phys.: Condens. Matter **18**, 11291 (2006).
[55] G. Kresse and J. Hafner, Phys. Rev. B **47**, 558 (1993).
[56] G. Kresse and J. Hafner, Phys. Rev. B **49**, 14251 (1994).
[57] G. Kresse and J. Furthmüller, Comput. Mater. Sci. **6**, 15 (1996).
[58] G. Kresse and J. Furthmüller, Phys. Rev. B **54**, 11169 (1996).
[59] G. Kresse and D. Joubert, Phys. Rev. B **59**, 1758 (1999).
[60] J. P. Perdew, K. Burke, and M. Ernzerhof, Phys. Rev. Lett. **77**, 3865 (1996).
[61] T. Saitoh, M. Nakatake, A. Kakizaki, H. Nakajima, O. Morimoto, Sh. Xu, Y. Moritomo, N. Hamada, and Y. Aiura, Phys. Rev. B **66**, 035112 (2002).
[62] H. J. Monkhorst and J. D. Pack, Phys. Rev. B **13**, 5188 (1976).
[63] R. D. Shannon, Acta Cryst. A **32**, 751 (1976).